World Journal of Engineering Research and Technology
WJERT
www.wjert.org
SJIF Impact Factor: 5.924

SUSTAINABLE PRODUCTION, MORPHOLOGICAL PROPERTIES AND SUCCESSFUL REMOVAL OF ANTIMICROBIAL ZINC NANOPARTICLES FOR ARTIFICAL WASTEWATER CONTAINING REACTIVE BLACK 5 (RB 5) SOLUTION

Ferda Gönen* and Gökhan Tekinerdoğan

Mersin University / Chemical Engineering Department / Çiftlikköy Mersin.

Article Received on 09/06/2023 **Article Revised on 29/06/2023** **Article Accepted on 19/07/2023**

***Corresponding Author**
Ferda Gönen
Mersin University / Chemical Engineering Department / Çiftlikköy Mersin.

ABSTRACT

In this study, the effect of environmental parameters such as pH, temperature, initial dye concentration and adsorbent concentration on the adsorption of synthetically prepared Reactive Black 5 (RB 5) dye solution to antimicrobial ZnF ($ZnFe_2O_4$) nanoparticles in a batch system was investigated. The amount of RB 5 adsorbed per unit adsorbent mass was determined as 97.48 mg $g^{-}L$ at T=45^{o}C and pH=2 value, the removal percentage was determined as 82.21% at these adsorption conditions. The kinetic, equilibrium and thermodynamic analysis of the system were carried out theoretically and experimentally, and the behavior of the adsorption system was interpreted with different equilibrium, thermodynamic and kinetic model equations. Temkin isotherm model has determined as the best repesentative model for RB 5-$ZnFe_2O_4$ adsorption system and the experimental kinetic data for the same adsorption system fits the second-order kinetic model. One of the reasons why antimicrobial Zn-based composite nanomaterial is preferred for the removal study is selectivity of nanoparticle. Another advantage of these nanoparticles is their fabrication suitability for multiple applications. The originality of this research is to investigate the treatatment wastewater containing RB 5 dye color and biological pollution together for the first time in literature.

KEYWORDS: Zn nanoparticles, RB 5, dye, removal, color, model.

1. INTRODUCTION

The presence of dye in wastewater originating from the textile industry is undesirable occasion in terms of aquatic life health as well as aesthetic appearance. The fact that modern synthetic dyes used in industrial processes cause an increase in pollution load due to a very stable structure and high concentration poses a great threat to the receiving environment in the discharge of wastewater[1-4] Therefore, the removal of these dyes included in the wastewater content has become a necessity for the sustainable and healthy use of limited resources in our country where water resources are increasingly depleted. For this purpose classical treatment methods that physical, chemical and biological methods are applied for the purpose of removing color from textile wastewater. Since most of the reactive dyes have a highly stable and carcinogenic structure, they cannot be decomposed and rendered harmless by biological treatment method, which is an effective technology for most pollutants.[2] In many studies, it has been determined that the biological processes are often insufficient because the amount and content of the textile industry wastewaters change unsteadily, frequently and violently. The limitations of the applicability of physical-physicochemical methods such as adsorption, coagulation, ion exchange, and the other traditional methods used in color removal, have been proven in most studies. In addition, some of the studies have proved that color cause color pollution in wastewater was removed by using the chemical coagulation process only by passing them from the aqueous phase to the solid phase without being exposed to any degradation.[2,5]

When the studies conducted in recent years are examined, there are a limited number of studies in which composite nanomaterials with magnetic and antimicrobial properties suitable for more than one application are used for color removal from wastewater. Some of these studies are summarized about magnetic or antimicrobial nanoparticles below . Ravindra Kumar Gautam et al. (2015) investigated the adsorption of malachite green (MG) and Congo red (CR) dyes with Fe-Zn nanoparticle synthesized by precipitation method. They have observed that the adsorption process can be represented by the Langmuir isotherm model, and the best model for the adsorption kinetic is pseudo-second-order kinetic model. The maximum adsorption capacities for MG and CR are found as 21.74 and 28.56 mg g^{-1}, respectively. Adsorption of these two dyes onto nanoparticles have positive $\Delta H°$ values of 62.73 and 69.65 kJ mol^{-1} for MG and CR, respectively, and $\Delta G°$ for all adsorption systems are negative.[6]

In 2017, Saima Farooq et al. investigated the adsorption of Crystal Violet (CV) dye on the synthesized $Ni05Co05Fe_2O_4$ nanocomposite material. In this study, it was observed that adsorption system reached equilibrium in 35 minutes of contact time. From the experimental results, pH value at which CV dye is maximally removed from aqueous solution was pH=11. At this pH value, initial dye concentration was 13.57 mg L^{-1}; the amount of adsorbent material was 0.089 g and the temperature was 22 ℃. At these conditions, the R^2 value 99.86% showed the satisfactory explanatory power of model.[7]

In 2014, Abbas afkhami et al. in 2014, synthesized Nickel-zinc ferrite ($Ni0._5Zn0.5Fe_2O_4$) nanocomposite material for the adsorption of Alizarin, Reactive Blue, Janus Green B, Congo Red, Crystal Violet and Methyl Violet dyes and Langmuir adsorption capacities (q_{max}) were determined as 250,0 mg g^{-1} for Alizarin, 333.3 mg g^{-1} for Reactive Blue and Janus green B, 500 mg g^{-1} for Congo red, Crystal Violet and Methyl Violet, respectively.[8]

In 2010, Xiangyu Hou et al. investigated the adsorption of Methylene Blue dye with particles synthesized by Sol gel method. It was determined that all samples showed high adsorption capacity and the removal efficiency of MB reached >90% within 3 hours.[9]

In 2011, Rahmatollah Rahimi synthesized zinc ferrite ($Zn\text{-}Fe_2O_4$) nanoparticles using ultrasonic waves, and used the nanoparticles to remove Congo Red (CR) dye color in wastewater. The maximum adsorption capacity of magnetic nanoparticles (0.02 g) was determined as 16.58 mg g^{-1} at 25 ℃ and pH 6, in the concentration range of 1-50 mg L^{-1}.[10]

In 2012, Niyaz Mohammad Mahmoodi, investigated the removal of Basic Blue 9 (BB9), Basic Blue 41 (BB41) and Basic Red 18 (BR18) dyes using magnetic nanoparticles (nickel-zinc ferrite), and examined the the equilibrium behaviour of adsorption and kinetics of process. At equilibrium, BB9, BB41 and BR18 adsorptions were determined as compatible with Tempkin and Langmuir isotherms, respectively. The maximum dye adsorption capacities (Q^0) of the nanoparticle were determined as 106 mg g^{-1}, 25 mg g^{-1} and 56 mg g^{-1} for BB9, BB41 and BR18, respectively.[11]

In this study, color removal from aqueous solution containing RB 5 dye by adsorption was investigated for the first time in the literatüre and researched magnetic and antibiotic (zinc-iron) ZnF ($ZnFe_2O_4$) nanomaterials in detail. Technically, the reasons of preference for ZnF ($ZnFe_2O_4$) nanoparticle were the particle selectivity, easy production and conservationist

production method compared to the most other synthesis adsorbents in this study. In addition, examination the simultaneous treatment of chemical and biological pollution together in dye containing wastewater with ZnF ($ZnFe_2O_4$) nanomaterials is the first step of an important treatment application for the real wastewater.

2. MATERIAL AND METHOD

2.1 Material

Iron(III) chloride ($FeCl_3$), Zinc chloride ($ZnCl_2$), Sodium hydroxide (NaOH) and Hydrochloric acid (HCl) used in adsorbent production and characterization experiments were obtained from Merck company and RB 5 dye was obtained from Sigma Aldrich company. *Bacillus subtilis*, *Klebsiella pneumoniae*, *Escherichia coli*, *Enterococcus fecalis* bacteria used during the color removal experiments to determine the antimicrobial activities of nanoparticles were supplied in Mersin University Biology Department Microbiology Laboratory by the assistance of responsible stuff.

2.2 Method

Equipments

Thermo Scientific Orion 5-Star Plus pH meter, Fourier transform Infrared Spectrophotometer (FT-IR), ZEISS Supra 55 model Field Emission Scanning Electron Microscope (FE-SEM), Sigaku, SmartLab model X-Ray Diffractometer (XRD), Shimadzu UV -1800 UV-Vis Spectrophotometer, WSB-30 Daihan brand shaking water bath, Protherm PLF 160/9 muffle furnace, Sigma 3-30K model centrifuge devices were used in adsorption experiments.

Preparation of $ZnFe_2O_4$ Nanoparticle

In the first step of the synthesis, 200 mL of 0.75 M ferric chloride ($FeCl_3$) and 200 ml of 0.25 M zinc chloride ($ZnCl_2$) solutions were prepared. Then, these two solutions were mixed and 2 M NaOH was added to the mixture at 60 ^oC on a magnetic stirrer to obtain pH 10 value. The final solution prepared was kept at 60 ^oC for 18 hours, then filtered and burned in a muffle furnace at 300 ^oC.[12] The obtained nanoparticle samples was broken into small pieces and their characterization was carried out using Field Emission Scanning Electron Microscope (FE-SEM), X-Ray Diffractometer and Fourier Transform Infrared Spectrophotometer (FT-IR) devices.

Determination of antimicrobial effect of nanoparticle

In this part, disk diffusion method was used to determine the antimicrobial effect of nanoparticles.[17-21] The basis principle of this method is to detect the inhibition area of the growth of microorganisms diffuses into the agar.To summarize the method, the formation of an open zone (the area where the microorganism could not grow) was detected around the holes in which $ZnFe_2O_4$-based nanomaterial was added at the end of the incubation period, Then the resulting zone diameters were measured in mm. The standard deviation of the zone diameters was calculated by performing all tests in 3 replicates.[13-17]

Color removal studies

Color removal experiments with synthesized nanoparticles were carried out in a batch system at constant temperature and constant shaking speed. The required amount of ZnF nanoparticles used in each experiment were mixed with 150 mL of dye solution (RB 5). (The pH of each solution was adjusted using NaOH and HCl solutions). Samples were taken from the flasks at 120 rpm in a shaking water bath at a predetermined time intervals for 0-1500 minutes, after centrifugation of the samples, appropriate dilutions were made and the last color of dye solution remaining without being adsorbed in the adsorption medium was determined by UV-Vis Spectrophotometer. Experiments were investigated by classical optimization method by keeping value of one parameter at constant magnitude and changing the other one within the specified range in order to examine the favorable adsorption values of pH, dye concentration, nanoparticle concentration and temperature.

3. RESULTS AND DISCUSSION

Adsorption Characterization Studies

SEM, FTIR and XRD Analysis Results

In RB 5 adsorption studies, it was observed that there was no change in the morphological structure of the surface of the nanoparticle, as it is seen from the SEM images before and after the adsorption. The absence of any change in the structure indicates that the adsorption takes place physically and there is no chemical bond formation.

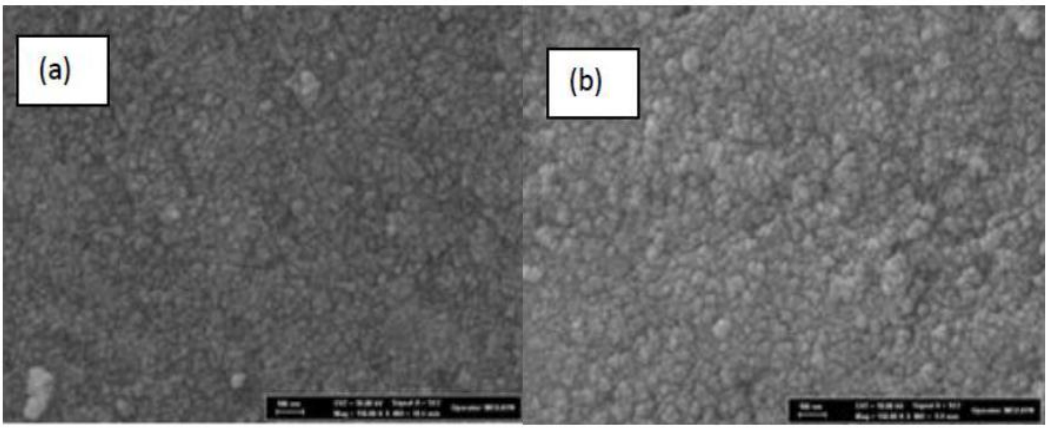

Figure 1: (a) $ZnFe2O_4$ based adsorbent before adsorption (b) $ZnFe_2O_4$ based adsorbent after adsorption with RB 5 (Experimental conditions: C=100 mg L^{-1}, T=25 C^o, Particle diameter=100 nm).

SEM images in Figure 1 reveal the stacked structure of the synthesized material. The size of the agglomerate is about 30 nm and they are connected to each other and form large structures. From the figure, a homogeneous structure is exhibited before and after adsorption.[18]

FT-IR analyzes were performed before and after adsorption for the nanoparticle to determine the adsorption mechanism in color removal of RB 5 solution. FT-IR studies carried out to determine the functional organic groups in the adsorbent were carried out in the frequency range of 500-4000 cm^{-1}.

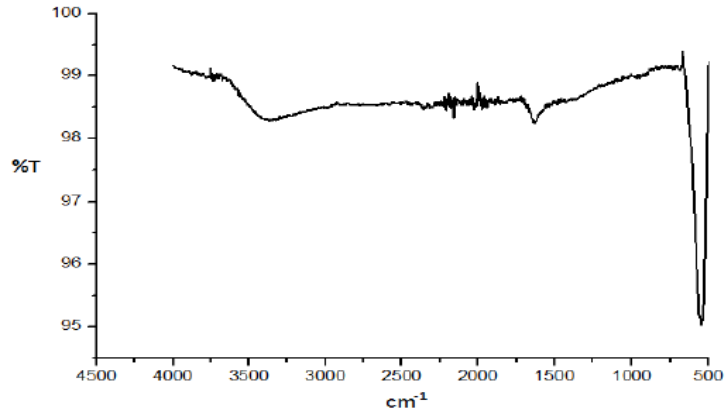

Figure 2: FTIR spectrum of ZnO ($ZnFe_2O_4$) based adsorbent before adsorption (Experimental conditions: C=100 mg L^{-1}, T=25 C^o, Particle diameter=100 nm).

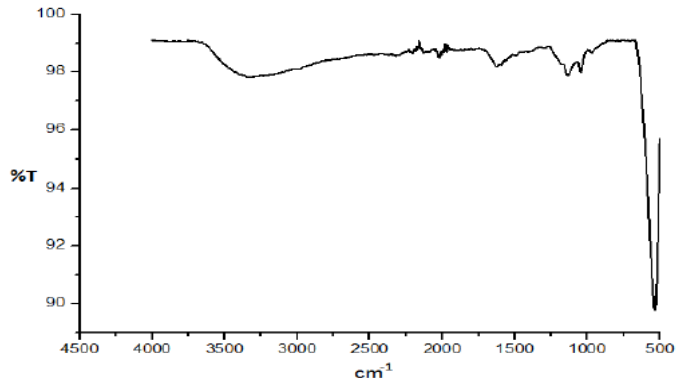

Figure 3: FT-IR spectrum of $ZnFe_2O_4$ based adsorbent after adsorption with RB 5 (Experimental conditions: C=100 mg L^{-1}, T=25 C^o, Particle diameter=100 nm).

The sharp peaks at 1040 and 1124 cm-1 of RB 5 seen in Figure 3 represent C-O bonds. The peak seen at 1625 cm-1 of $ZnFe_2O_4$ +RB 5 comes from adsorbent $ZnFe_2O_4$ and the peaks at 1040, 1124cm-1 come from RB 5 dye. It is observed that after the interaction of the Fe-O bond in $ZnFe_2O_4$ with the dye, the dye binds from oxygen and shifts at a peak wavelength of 500-600 cm^{-1}. It was understood from the FT-IR results that the dye molecules has coated the adsorbent surface completely (adsorption process).

In the XRD analysis performed to examine the phases and crystal structure of the $ZnFe_2O_4$-based adsorbent used in the adsorption studies of the RB 5 dye, it was observed that the $ZnFe_2O4$-based nanomaterial had a cubic crystal structure and after adsorption, the cubic crystal structure did not change as seen in the figure [19] As a result of the XRD analysis, the simple formula of the material was found to be $ZnFe_2O_4$. has been determined.

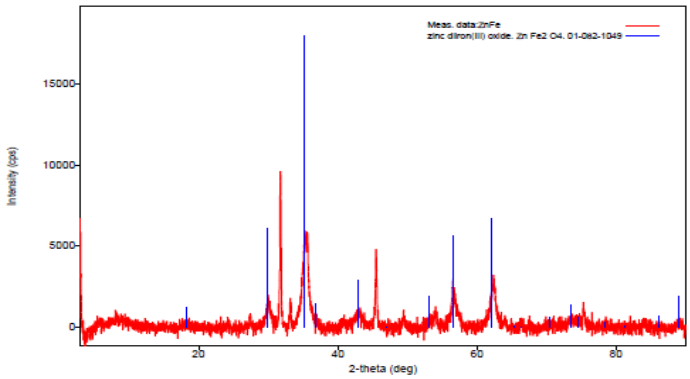

Figure 4: XRD spectrum of $ZnFe_2O_4$ based adsorbent before adsorption (Experimental conditions: C=100 mg L^{-1}, T=25 C^o, Particle diameter=100 nm).

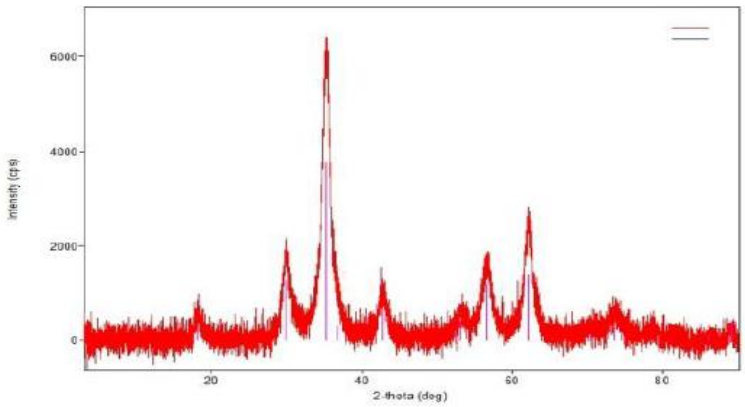

Figure 5: XRD spectrum of $ZnFe_2O_4$ based adsorbent after adsorption (Experimental conditions: C=100 mg L^{-1}, T=25 C^o, Particle diameter=100 nm).

Determination of the antimicrobial effect of nanoparticle

When the literature is reviewed, it is found that ZnF-based nanomaterials have high antimicrobial property. This part of the investigation is related with the determination of the antimicrobial effect of the ZnF-based nanoadsorbent. In this experimental part, the antimicrobial properties of ZnF-based nanomaterials produced by the hole agar difufusion method were determined by the cavity diffusion methodology with two different Gram-positive (*Bacillus subtilis and Enterococcus fecalis*) and two Gram-negative (*Escherichia coli and Klebsiella pneumoniae*) bacteria. The inhibition areas observed for *Bacillus subtilis, Enterococcus fecalis, Escherichia coli, and Klebsiella pneumoniae bacteria* with the susceptibility test are shown in Table 1 (field area size) and in Figure 6-9 (images). From the experimental results, it can be said that ZnF based nanomaterials have antimicrobial property to the antimicrobial effect of four different bacteria at various adsorbent doses. When the experimental data was evaluated, it was seen that the inhibition zones were observed at 25 mg L^{-1}, 50 mg L^{-1}, and 75 mg L^{-1} dosages for *E. coli*; at 50 mg L^{-1} and 75 mg L^{-1} dosages for Bacillus subtilis and *Enterococcus fecalis bacteria*; and at 75 mg L^{-1} dosage for *Klebsiella pneumoniae* bacteremia.

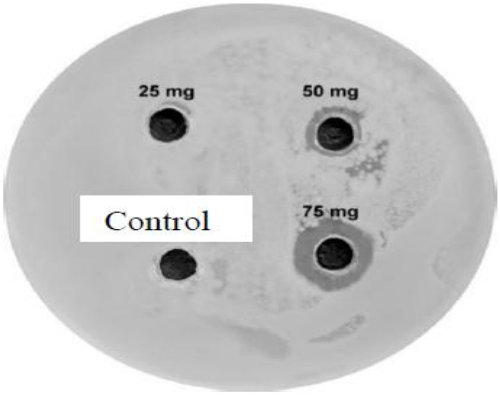

Figure 6. Determination of the antimicrobial effect of $ZnFe_2O_4$-based nanomaterial on *Bacillus subtilis* by diffusion susceptibility method (Experimental conditions: T=25 ^oC, Particle diameter=100 nm).

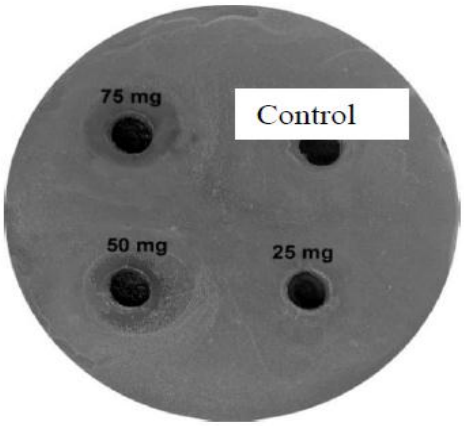

Figure 7: Determination of the antimicrobial effect of $ZnFe_2O_4$ based nanomaterial on *E.fecalis* by diffusion susceptibility method (Experimental conditions: T=25 ^oC, Particle diameter=100 nm).

Figure 8: Determination of the antimicrobial effect of $ZnFe_2O_4$-based nanomaterial on *E.coli* by diffusion susceptibility method (Experimental conditions: ^oT=25 C, Particle diameter=100 nm).

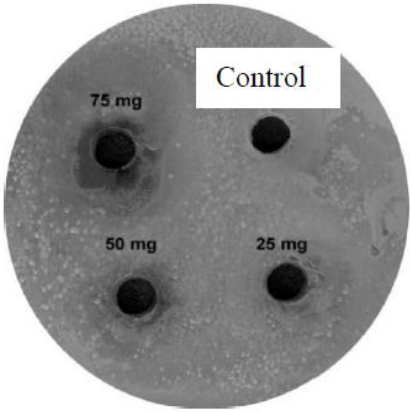

Figure 9: Determination of the antimicrobial effect of $ZnFe_2O_4$-based nanomaterial on *K. pneumoniae* by diffusion susceptibility method (Experimental conditions: T=^{o}25 C, Particle diameter=100 nm).

Table 1: Inhibition zones observed as a result of diffusion susceptibility test.

Type of bacteria	Amount of substance added (mg)	Inhibition zone diameter (mm)
Bacillus subtilis	25	-
	50	11
	75	15
Enterococcus fecalis	25	-
	50	13
	75	18
Escherichia coli	25	14.5
	50	18
	75	21
Klebsiella pneumoniae	25	-
	50	10
	75	16.5

As a result of the experimental studies, ZnF-based nanomaterials have superior advantage of advanced antimicrobial property against many harmful pathogens besides ecofriendly color removal.[28–31]

Determination of favorable conditions for adsorption

In order to observe the effect of pH parameter in the adsorption of RB 5 dye on $ZnFe_2O_4$ based nanomaterials, the initial pH value was changed in the range of 2-10 while the initial dye concentration, temperature, adsorbent concentration were kept constant at (100 mg L^{-1}), (25°C) and (1g L^{-1}), respectively. According to the obtained results, maximum color removal was observed at pH 2 value at constant adsorption parameters [Figure 10]. When the charges

of nanoadsorbent and dye solution in adsorption was investigated, it was seen that RB 5 dye used in adsorption studies was anionic and nanoadsorbent surfaces were cationic characteristics. Since the electrostatic interaction between the positively charged adsorbent and the dye anions, the adsorption capacity of the adsorbent reached the maximum value at pH=2 value. At pH=7 (isoelectric point), and above this pH values, nanoadsorbent surface became negatively charged, electrostatic repulsion occurred between the adsorbent surface and the dye anions, and the dye removal decreased sharply.[20,21]

In the adsorption of RB 5 dye to $ZnFe_2O_4$ based nanomaterial, in order to investigate the effect of initial dye concentration; the initial dye concentration values were changed in the range of 25–2000 mg L^{-1} pH, temperature and adsorbent concentration values were kept constant at (2.0), (25 ^oC) and (1.0 g L^{-1}), respectively. When the experimental results were examined, it was observed that the amount of adsorbed dye concentration increased with the increase of the initial dye solution concentration and the equilibrium time for the adsorption system [Figure 11]. In the adsorption of RB 5 dye, when the initial dye concentration was increased from 25 mg L-1 to 500 mg L^{-1}, the amount of dye adsorbed in the unit adsorbent mass at equilibrium increased from 25 mg g-1 to 90.79 mg g-1, respectively. For the same adsorbent-adsorbate system, complete removal was observed at the initial dye concentration of 25 mg L^{-1} at 360 minutes, equilibrium time is about 1500 minutes at higher initial dye concentration.

In order to investigate the effect of temperature on adsorption equilibrium, the temperature values were examined at 25, 35, 45, 55 °C while the initial pH value, initial dye concentration, adsorbent concentration was kept constant at 2.0, 100 mg L^{-1} and 1.0 g L^{-1}, respectively. From the experimental results, it was found that temperature value of the highest removal yield was 45 ^oC observed for the adsorption of RB 5 dye to $ZnFe_2O_4$.

At the last step, adsorbent dose was studied by changing nanoparticle dosage in the range of 0.2–3.0 g L^{-1} while the other adsorption parameters were kept constant at pH value of 2, initial dye concentration of 100 mg L-1, and temperature of 45 ^oC. In adsorption process, as the adsorbent dose increases, the amount of adsorbed material decreases as a result of the interaction of the adsorbent particles and the formation of adsorbent pellet by flocculation of the nanoparticles [Figure 12]. In addition, % removal values were increased with the increasing the adsorbent dose. This phenomena was explained by the increase in the number

of dye molecules that will adhere to this surface area with the increase in the adsorbent contact surface area.[19]

As a result of the adsorption experiments, the favorable adsorption conditions were determined as pH value of 2, temperature of 45°C, and the adsorbent dose of 1.0 g L^{-1}.The amount of dye adsorbed per unit adsorbent mass in equilibrium of 97.48 mg g^{-1}, and the percentage color removal of 82.21% at this favorable conditions.

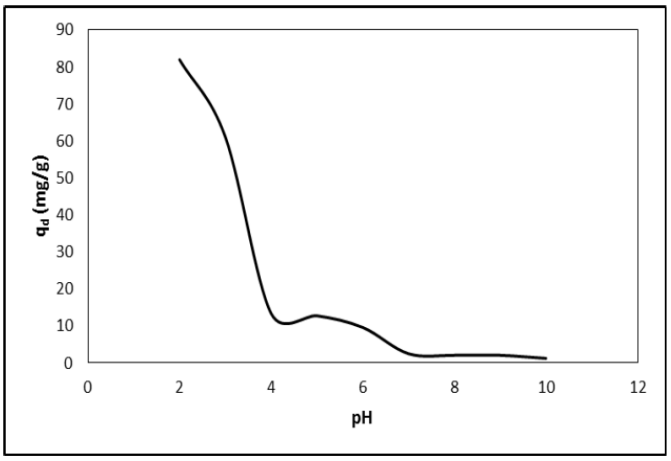

Figure 10: The effect of initial pH on the adsorption of RB 5 dye to ZnF-based nanomaterials (initial dye concentration: 100 mg L^{-1}; adsorbent concentration: 1g L^{-1}; temperature: 25°C).

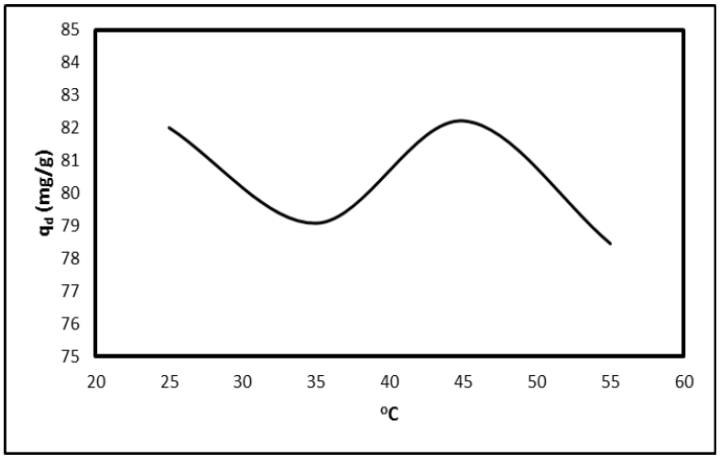

Figure 11: The effect of temperature on the adsorption of RB 5 dye to ZnF-based nanomaterials (initial dye concentration: 100 mg L^{-1}; initial pH: 2.0 adsorbent concentration: 1.0 g L^{-1}).

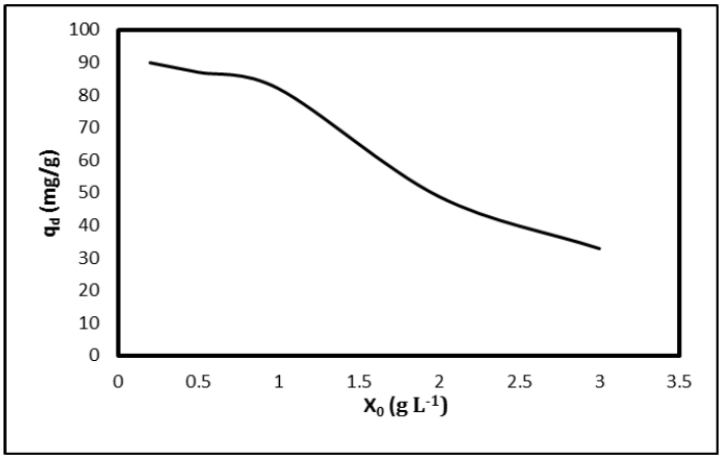

Figure 12: The effect of different ZnF-based adsorbent concentrations on the amount of RB 5 dye adsorbed at equilibrium (initial dyeconcentration: 100 mg L^{-1}; initial pH:2.0; temperature: 25℃).

Adsorption Equilibrium and Isotherm models

Langmuir, Freundlich, and Temkin isotherm models were tested in order to determine the isotherm model equation best fitted to the experimental equilibrium data obtained at different temperatures with the highest agreement in the adsorption of RB 5 dye to the $ZnFe^2O_4$-based nanomaterial; the obtained results are presented below.[23-27, 29-32]

Langmuir ısotherm model

RB 5-$ZnFe_2O_4$ equilibrium data for the adsorption system was examined with the help of the linear form of the Langmuir isotherm model.[24,25,26] Model constants (Q^o and b) were calculated from the slopes and shifts of the obtained linear model graphs; and the constants and R2 values are given in Table 2.

Table 2: Langmuir isotherm model constants for the adsorption of RB 5 dye to $ZnFe_2O_4$-based nanomaterial.

T (°C)	25°C	35 °C	45 °C	55 °C
Q° (mg mg^{-1})	84.03	82.64	95.23	88.49
b (L mg^{-1})	3.40	7.11	0.53	0.64
R^2	0.936	0.886	0.942	0.872
R_L	0.0029	0.0014	0.0183	0.0153

As it seen from Table 2, it is seen that the R2 values are quite high. Calculated dimensionless separation factors (RL) range from 0 to 1. As a result, it can be said that the adsorption system is compatible with the Langmuir isotherm model.

Freundlich ısotherm model

In order to determine the suitability of Freundlich isotherm model for the multilayer adsorption equilibrium data for RB 5 dye onto $ZnFe_2O_4$-based nanomaterial, linear form of the Freundlich model was used for the adsorption system [24, 25, 26]. Model constants (n and Kf) were determined from linear Freundlich isotherms slope and shift; constants and R2 values are presented in Table 4.3.

Table 3: Freundlich isotherm model constants obtained at different temperatures in the adsorption of RB 5 dye to $ZnFe_2O_4$-based nanomaterial.

T (°C)	25 °C	35 °C	45 °C	55 °C
1/n	0.0782	0.076	0.072	0.062
n	12.78	13.03	13.774	1594
Kf [(mg/g)/(L/mg)$^{1/n}$]	11521.26	11700.38	14461.05	14015.22
R^2	0.893	0.968	0.961	0.972

It is seen that the regression coefficients (R2) values are quite high in the Freundlich Isotherm model. It is observed that the calculated "n" values are greater than 1, and accordingly, the adsorption system can be represented with Freundlich isotherm model.

Temkin ısotherm model

Equilibrium data of RB 5- $ZnFe_2O_4$ adsorption were examined with the help of linear form of Temkin isotherm model [24, 25, 26]. Temkin isotherm model constants were calculated from linear Temkin isotherm model constants and R2 values are given in Table 4.

Table 4: Temkin isotherm model constants obtained at different temperatures in the adsorption of RB 5 dyestuff to $ZnFe_2O_4$-based nanomaterial.

T (°C)	25 °C	35 °C	45 °C	55 °C
A_t (L g^{-1})	113.64	124.11	66.59	156.67
B (J mol^{-1})	12.44	12.21	14.02	11.65
R^2	0.92	0.983	0.97	0.97

From the table, it is seen that R2 values are quite high according to the results of the applied Temkin Isotherm model. Accordingly, it is seen that the adsorption system can be represented successfully with Temkin isotherm model.

When all three isotherm models were investigated for the representative adsorption isotherm model for RB 5 dye on $ZnFe_2O_4$-based nanomaterial, although it was found that all the

equilibrium adsorption data was compatible with Langmuir, Freundlich and Temkin isotherm models it was observed that the best fit was achieved with the Temkin isotherm model.

Adsorption kinetics

Pseudo first order kinetic model

In order to model the adsorption kinetics, the compatibility of the experimental data obtained at different initial dye concentrations to the pseudo first order kinetic model was investigated [24, 27]. The pseudo first order rate constant values obtained from the straight slopes of the RB-$ZnFe_2O_4$ adsorption system are presented in Table 5 with the R2 (regression coefficient) values.

Table 5: Pseudo first order rate constant and R2 (Regression coefficient) values of the adsorption of RB 5 dye to $ZnFe_2O_4$ based nanomaterial.

C_o (mgL^{-1})	$q_{d,deneysel}$ ($mg\ g^{-1}$)	$q_{d,hesaplanan}$ ($mg\ g^{-1}$)	$k_1(dk^{-1})$	R^2
25	25.00	20.32	0.02740	0.990
50	50.00	58.53	0.02095	0.964
75	69.97	51.47	0.00690	0.970
100	82.21	59.67	0.00483	0.955
200	89.53	46.14	0.00345	0.953
300	96,23	56.02	0.00345	0.975
400	96.23	55.96	0.00322	0.944
500	97.48	53.83	0.00322	0.939

It is seen from the table that the R2 values for the nanoparticle-RB 5 dye system are quite high. But, the fact that a great difference between experimental qd values and the theorotical ones is the proof of unconformity to the pseudo first order kinetic model.

Pseudo second order kinetic model

In order to investigate the kinetics of adsorption of RB 5 dye on $ZnFe_2O_4$ based nanomaterial, the experimental data obtained in the equilibrium state were analyzed by pseudo second order kinetic model equation.[27, 29-33]

The rate constant values obtained from the pseudo-second order kinetic model graphs were determined and the results are presented in Table 6 together with the R2 (regression coefficient) values.

Table 6: Pseudo second order rate constant and R2 (Regression coefficient) values of the adsorption of RB 5 dye on $ZnFe_2O_4$ based nanomaterial.

C_o (mgL^{-1})	$q_{d,deneysel}$	$q_{d,hesaplanan}$	$k_2(g(mgmin)^{-1})$	R^2
25	25.0	25.12	0.006578	1.00
50	50.0	50.76	0.000907	0.999
75	69.97	71.42	0.000424	0.999
100	82.21	84.03	0.000243	0.999
200	89.53	90.90	0.000121	0.999
300	96.23	99.00	0.000215	0.999
400	96.23	99.00	0.000196	0.998
500	97.48	100.0	0.000215	0.999

From Table 6, it can be said approximately that, the equality of experimental qd values and the theorotical ones with high R2 values of the RB 5 dye at high concentrations proved that Pseudo second order model is the best representative model fort he adsorption system.

Adsorption thermodynamics

Thermodynamic parameters such as Gibbs free energy change (ΔG), enthalpy change (ΔH) and entropy change (ΔS) were calculated according to the Van't Hoff equation in order to perform the thermodynamic analysis of the RB 5-$ZnFe_2O_4$ adsorption system [26-30]. Values such as Gibbs free energy change (ΔG), enthalpy change (ΔH) and entropy change (ΔS) belonging to thermodynamic analysis are presented in the Table below, respectively.

Table 7: Thermodynamic parameters calculated using Van't Hoff equation for the adsorption of RB 5 dye to $ZnFe_2O_4$ based nanomaterial.

T(K)	ΔG(J mol^{-1})	ΔH(kJ mol^{-1})	ΔS(J $mol.K^{-1}$)	TΔS(J mol^{-1})
298	-6121.39			32671.73
308	-7462.05	26.471	109.6367	33768.10
318	-8303.27			34864.47

As it seen fromTable 7, Gibbs free energy change (ΔG) values are nagative, enthalpy change (ΔH) and entropy change (ΔS) values are positive, and according to the analysis results, it is clearly observed that the RB 5-$ZnFe_2O_4$ system is an endothermic and spontaneous adsorption system.

4. CONCLUSION

As a result of the experimental studies carried out, optimum pH and temperature decolorization parameters were determined as pH= 2.0, and T=45 ^oC in the adsorption of RB 5 dye on $ZnFe_2O_4$ based nanomaterial. The amount of dyes adsorbed per unit adsorbent mass

in equilibrium and the percentage of removal in equilibrium were determined as 97.48 mg dye/g adsorbent and 82.21% at favorable adsorption. Looking at the literature, Sheshdeh et al. (2014) investigated the adsorption of Basic Red 46 (BR46) aqueous solution to inexpensive diatomite-modified nickel oxide nanoparticles (NONMD) in a batch system. The maximum percentage of BR46 removal from the aqueous solution was found to be 99.48% under the conditions where the temperature was 25 ^{o}C, pH 8, stirring speed 200 rpm, initial dye concentration 25 mg L^{-1} and mixing time 60 minutes.

In characterization studies, it can be seen from the SEM images, there is no change in the morphological structure of the nanoparticle surface used, so the adsorption takes place physically; It was observed that the peaks in the FT–IR spectra obtained before adsorption of the adsorbent shifted slightly compared to the peaks obtained after adsorption. As a result of XRD analysis, it was determined that the synthesized nanomaterial had the simple formula of ZnF ($ZnFe_2O_4$).

In antimicrobial activity studies, the antimicrobial properties of ZnF-based nanomaterial with a total of 4 different bacteria, 2 Gram positive (*Bacillus subtilis and Enterococcus fecalis*) and 2 Gram negative (*Escherichia coli and Klebsiella pneumoniae*), were determined by space diffusion method. In the study conducted with *E.coli* bacteria, an inhibition zone was observed at 25 mg, 50 mg and 75 mg doses, while an inhibition zone was observed for *Bacillus subtilis* and *Enterococcus fecalis* at 50 mg and 75 mg doses, and for *Klebsiella pneumoniae* at a dose of 75 mg.

It has been observed that the adsorption equilibrium data obtained at different temperatures in the adsorption of RB5 dye to $ZnFe_2O_4$-based nanomaterial are best represented with the Temkin isotherm model. In the literature, Patra et al. (2016) investigated the removal of cationic dyes (methylene blue, MB and rhodamine B, RhB) by synthesizing a highly efficient and fast monometallic/bimetallic nanoparticle modified polysaccharide (agar) based adsorbent. In this study, due to the different surface interaction between the dye-nanoadsorbent, the adsorption equilibrium was compatible with Freundlich isotherm model .

In the adsorption kinetic calculations, it was determined that the adsorption system could be represented by the second order kinetic model due to the high regression coefficient values and it was noticed that the equality of experimental qd values with the calculated theorotical qd values. When the literatüre is searched, similar to this study, Nassar et al. (2016)

investigated the adsorption properties of MgO particles for the removal of Reactive Red 195 (RR195) and Orange G (OG) anionic dyes. From the experimental results, it was stated that the adsorption data were expressed by the pseudo-second-order kinetic model.

In the thermodynamic calculations, it was determined that the ΔH (26.471 kJ mol^{-1}) and ΔS value for the adsorption of the RB 5 dye were positive and the ΔG value was negative, in other words, it was a spontaneous and endothermic adsorption system. In literatüre, Ravindra Kumar Gautam et al. used a different dye-adsorbent system. The adsorption process with Fe-Zn nanoparticles to malachite green (MG) and Congo red (CR) dyes is endothermic (62.73 and 69.65 kJ $mol^{-1,}$ for MG and CR) and They stated that ΔG° values for all processes are negative, that is, they occur spontaneously. Similarly, Farideh Dehghani et al. showed in 2016 that the adsorption of BPR (bromophenol red) onto synthesized $CoFe_2O_4$, $ZnFe_2O_4$ and $NiFe_2O_4$ nanoferrite particles is endothermic and self-executing.

As a result of the experimental study, it was observed that the synthesized $ZnFe_2O_4$-based nanomaterial was used with a very high efficiency in color removal from synthetic wastewater solution containing RB 5 textile dye. The most important advantage of adsorbent nanomaterial used in this adsorption study is antimicrobiality for microbial growth, This advantage of the nanoparticle is the main reason why the synthesized nanomaterial is preferred for successful use in color removal from textile industry wastewater containing color and microbial contamination at the same time. In real wastewater systems, many types and amounts of pollutants (heavy metals, phenol, phosphorus, oil, etc.) can coexist in wastewater in addition to microbial contamination.

ACKNOWLEDGEMENT

Assoc. Prof. Dr. Ferda Gönen thankfully acknowledges Mersin University Scientific Research Unit which provided financial support to the experimental studies within the scope of the Master's Thesis Project No. 2017-1-TP 2-2266, Mersin University Advanced Technology Education, Research and Application Center. We would like to thank the Microbiology Laboratory of the Department of Biology and its staff.

REFERENCES

1. Rajeev J & Meenakshi S Photocatalytic removal of hazardous dye cyanosine from industrial waste using titanium dioxide, Journal of Hazardous Materials, 2008; 152 (1): 216–220.

2. Kaur S and Singh V "TiO_2 mediated photocatalytic degradation studies of Reactive Red 198 by UV irradiation" Journal of Hazardous Materials, 2007; 141 (1): 230–236.
3. Ğassan A Onur B "Investigation of the Effect of Raising and Finishing Process on the Physical Performance of 3-Thread Fleece Fabric" Tekstil ve Konfeksiyon Dergisi, 2022; 32(3): 183 – 192.
4. Sena DG Sennur AA. "Development of Temperature and pH Responsive Smart Cotton Fabrics by P(NIPAM–co-MAM) Copolymer Finishing" Tekstil ve Konfeksiyon Dergisi, 2022; 32(3): 193 – 207.
5. Vijayaraghavan G & Shanthakumar S. "Effective removal of reactive magenta dye in textile effluent by coagulation using algal alginate, Desal. Water Treat, 2018; 121: 22–27.
6. Ravindra KG Vandani R Sushmita B Maria AS Shivani S Sanjeev KS Banerjee MA Sanroman S. Soni Mahesh CC, "Synthesis of bimetallic Fe-Zn nanoparticles and its application towards adsorptive removal of carcinogenic dye malachite green and Congo red in water Journal of Molecular Liquids", 2015; 212: 227-236.
7. Saima F Abubakr S Muhammad S Javid H Fazal M Maryam İ. Process optimization studies of crystal violet dye adsorption onto novel, mixed metal $Ni_{0.5}Co_{0.5}Fe_2O_4$ ferrospinel nanoparticles using factorial design Journal of Water Process Engineering, 2017; 16: 132-141.
8. Abbas A, Shadieh S, Razieh M, and Tayyebeh M. Magnetic nickel zinc ferrite nanocomposite as an efficient adsorbent for the removal of organic dyes from aqueous solutions Journal of Industrial and Engineering Chemistry, 2015; 21: 920-924, 2015.
9. Xiangyu H, Jing F, Xiaohan L, Zhuangjun F, Milin Z. Hou J. Feng X. Liu Y. Ren Z. Fan M Zhang Magnetic and high rate adsorption properties of porous Mn1-xZnxFe2O4 ($0 \leq x \leq 0.8$) adsorbents Journal of Colloid and Interface Science, 2011; 353 (2): 524–529.
10. Rahmatollah R, Hamed K, Mahboubeh R, Shafiee M. Synthesis, characterization and adsorbing properties of hollow Zn-Fe_2O_4 nanospheres on removal of Congo red from aqueous solution Desalination, 2011; 280 (1–3): 412–418.
11. Mahmoodi NM, "Magnetic ferrite nanoparticle-alginate composite: Synthesis, characterization and binary system dye removal" Journal of the Taiwan Institute of Chemical Engineers, 2013; 44 (2): 322–330.
12. Sujata M & Subramarian N, "Adsorption and catalytic degradation of organic dyes in water using ZnO/$Zn_xFe_{3x}O_4$ mixed oxides" Journal of Environmental Chemical Engineering", 2015; 3: 1185–1193.

13. Lyudmila B Galina G Rossen N Sirigan D Elegan L Nikolai K İvan M Zacharii K. "Activity of Bulgarian propolis against 94 Helicobacter pylori strains in vitro by agar-well diffusion, agar dilution and disc diffusion methods" Journal of Medical Microbiology, 2005; 54 (5): 481–483.
14. Gökhan T, Manyetik ve antimikrobiyal özellikli çinko-demir (ZnF) bazlı nanoparçacıklar ile atıksulardan renk gideriminin incelenmesi: Renk giderim mekanizmasının araştırılması, Yüksek Lisans Tezi, Mersin Üniversitesi Fen Bilimleri Enstitüsü. Mersin, 2017.
15. Soner A Ali Osman A Burhan Ş Munir T & Hülya MG Effects of bacteria on CdS thin films used in technological devices Materials Research Express, 2017; 4(4): 046402.
16. Rajeshwari S Pattanathu KSMR Rajiv P Hasna AS Venckatesh R, Biogenic copper oxide nanoparticles synthesis using Tabernaemontana divaricate leaf extract and its antibacterial activity against urinary tract pathogen Spectrochimica Acta - Part A: Molecular and Biomolecular Spectroscopy, 2014; 133: 178–181.
17. Peter L Sivagnanam S Jayanthi A, Synthesis of silver nanoparticles using plants extract and analysis of their antimicrobial property Journal of Saudi Chemical Society, 2015; 19 (3): 311–317.
18. Wojciech K Daniel S Ewa M Zofia LB Ursula N, "Equilibrium and kinetic studies on acid dye Acid Red 88 adsorption by magnetic ZnF ($ZnFe_2O_4$) spinel ferrite nanoparticles" Journal of Colloid and Interface Science, 2013; 398: 152–160.
19. Nevine KA, Removal of Reactive Dye from Aqueous Solutions by Adsorption Onto Activated Carbons Prepared from Sugarcane Bagasse Pith Desalination, 2008; 223(1); 152-161.
20. Nour TAG El-Shaimaa AR El-Chaghaby G, Equilibrium and kinetic study for the adsorption of p-nitrophenol from wastewater using olive cake based activated carbon Global J. Environ. Sci. Manage, 2016; 2(1): 11-18.
21. Felix AA Andrew NA Albert IA "Batch study, equilibrium and kinetics of adsorption of naphthalene using waste tyre rubber granules Journal of Xenobiotics", 2014; 4, 2264: 20-27.
22. Junixiong L & Lan W, "Comparison between linear and non-linear forms of pseudofirst-order and pseudo-second-order adsorption kinetic models for the removal of methylene blue by activated carbon" Environ. Sci. Engin. China, 2009; 3(3): 320–324.

23. Maryam G Nahid G Gholamreza Z Sharifah RWA, Kinetic and equilibrium study of Ni(II) sorption from aqueous solutions onto Peganum harmala-L Int. J. Environ. Sci. Technol, 2014; 11: 1835–1844.
24. Yuen SH Gordon M "Pseudo-second order model for sorption processes Process Biochemistry", 1999; 34: 451–465.
25. Mujgan O, "Tekstil Atıksularındaki Metal Kompleks Boyarmaddelerin Yumurta Kabukları İle Giderimi" Gazi Üniversitesi, Gazi Üniv. Müh. Mim. Fak. Der, 2013; 28: 777-785.
26. Ramazan C Serpil S Ali D, "Adsorption properties of activated almond shells for methylene blue (MB)" Environmental Research & Technology, 2018; 1 (2): 31-38.
27. Rakesh G Damodar RD, "Tobacco stem ash as an adsorbent for removal of methylene blue from aqueous solution: Equilibrium, kinetics, and mechanism of adsorption" Water. Air. Soil Pollut, 2013; 224: 6.
28. Alan LM, "Thermodynamics of adsorption" Chemical Thermodinamics for Industry, 2004; 47: 243–252.
29. Seyed MM Soheil KN Mohammad P Nima A "Methylene blue adsorption via Maize Silk Powder: Kinetic, Equilibrium, Thermodynamic Studies and Residual Error Analysis Process Saf. Environ. Prot, 2017; 106: 191–202.
30. Reza KS Mohammad RKN Khashayar B Nargess YL Gelayol G, "Equilibrium and kinetics studies for the adsorption of Basic Red 46 on nickel oxide nanoparticles-modified diatomite in aqueous solutions" Journal of the Taiwan Institute of Chemical Engineers, 2014; 45: 1792–1802.
31. Santanu P Ekta R Rashmi M Prashant KS, "Agar based bimetallic nanoparticles as high-performance renewable adsorbent for removal and degradation of cationic organic dyes Journal of Industrial and Engineering Chemistry", 2015; 33: 226–238.
32. Mostafa YN Talaat YM İbrahim SA Ihab S, "MgO nanostructure via a sol-gel combustion synthesis method using different fuels: An efficient nano-adsorbent for the removal of some anionic textile dyes" Journal of Molecular Liquids, 2017; 225: 730-740.
33. Ravindra KG Vandani R Sushmita B Maria AS Shivani S Sanjeev KS Mahesh CC, "Synthesis of bimetallic Fe-Zn nanoparticles and its application towards adsorptive removal of carcinogenic dye malachite green and Congo red in water" Journal of Molecular Liquids, 2015; 212: 227–236.